

Perspective

Scaling up high-energy-density sulfidic solid-state batteries: A lab-to-pilot perspective

Darren H.S. Tan,^{1,*} Ying Shirley Meng,^{1,2,*} and Jihyun Jang^{1,*}

SUMMARY

Recent years have seen monumental and exciting developments in the field of all-solid-state batteries (ASSBs). Despite its promises, they still face a multitude of technical hurdles before commercialization can be achieved. Among these challenges, none are more daunting than the ability for scale-up prototyping, specifically, enabling technology transition from the laboratory to the pilot scale. A vast majority of ASSB reports to date are still limited to form factors impractical for actual device operation. Here, we provide a perspective on a wide range of scalability challenges and considerations for ASSBs, including solid electrolyte synthesis, dry electrode and separator processing, cell assembly, and stack pressure considerations at the module level. We layout baseline protocols for ASSB fabrication and evaluation using pouch-cell-type form factors as a baseline. Finally, we discuss ways to bridge the development gap between university-level research and industry-scale production through partnerships with national laboratories.

INTRODUCTION

The development of all-solid-state batteries (ASSBs) has seen tremendous progress in recent years, owing to the discovery of highly conductive and stable inorganic solid-state electrolyte (SSE) materials.^{1,2} These include a broad-spectrum of material classes including but not limited to oxides,³ sulfides,⁴ borohydrides,⁵ and halide-⁶ type materials, some of which have demonstrated room temperature Li⁺ ionic conductivities exceeding that of conventional liquid electrolytes (>10 mS/cm).⁷ This has directly resulted in numerous major breakthroughs in enabling next-generation electrode materials, such as Li metal and Li-alloy anodes, and ultra-high Ni cathodes, demonstrating clear pathways toward the promise of high energy densities unachievable by conventional lithium-ion batteries (LIBs).^{8–10} Beyond energy density improvements, ASSBs are widely believed to overcome various fundamental obstacles faced by conventional LIBs. These include lowered costs per kWh, improved safety due to its intrinsic non-flammability, a wider operating temperature range, as well as increased longevity due to the self-passivating properties of electrode-electrolyte interfaces formed.¹¹

In the literature, there are two major classes of solid-state batteries commonly reported, “all-solid-state” versus “solid-state” batteries, with the former defined as being entirely solid in nature, whereas the latter commonly refers to liquid-solid hybrids where organic liquid electrolytes, polymeric-gels, or salt-in-liquid type electrolytes are used in the cell in combination with a polymer-oxide separator.^{12,13} Although the “all-solid-state” classification of batteries can be clearly defined by their intrinsic material chemistries used (e.g., no liquids), the boundaries for “solid-state” batteries tend to be blurred. Without clear definitions of what

CONTEXT & SCALE

The discovery of highly conductive solid electrolyte materials has fueled numerous exciting developments within the all solid-state battery field. However, the question of its processing scalability and transition toward pilot-scale prototyping still remains largely unanswered. In this perspective, we discuss a range of scalability considerations for all solid-state batteries and summarize promising solutions to overcome these challenges through experimental proofs of concepts. Overall, this perspective seeks to engender greater research focus toward scalability and manufacturability often overlooked within the field of all solid-state batteries.

constitutes a solid-state battery, it becomes challenging to identify and therefore allocate resources toward promising development pathways that result in meaningful advancements to the technology. One possible confusion arises from the amount of liquid electrolyte excess used in the liquid-solid hybrid batteries. In previous “solid-state” battery studies, impressive cell performance data were reported using liquid electrolytes but without reporting the amounts used or using amounts that exceed quantities used in LIBs,^{14–19} calling into question whether the proposed chemistry is more like a modified LIB versus a “solid-state” battery. Granted, use of liquid-solid hybrids presents significantly lower barriers for entry due to its similarity and compatibility with LIB prototyping processes. However, this potentially diminishes the prospects of improved safety, energy density, and thermal and interfacial stabilities necessary for emerging applications such as electric vehicles and stationary grid storage.²⁰

Although ASSBs offer the capability to maximize the aforementioned metrics, they present a much higher barrier to entry and, more crucially, barriers toward scaling up from the laboratory to pilot and finally to production scale. Critics have also cited long timelines toward commercialization, along with the multifarious scientific and engineering hurdles associated with its processing challenges to characterize ASSBs as hype and being unable to displace LIBs anytime soon.^{20,21} Indeed, LIBs today have largely dominated the global consumer electronics markets. However, the promise of ASSBs do not necessarily seek to compete in such markets. Similarly, the advent of LIBs did not eradicate the lead acid battery or the primary alkaline battery markets but enabled new applications in portable devices that could not be realized with prior technologies. Therefore, ASSBs are believed to open new market segments previously underserved by LIBs. In terms of timelines to market, ASSBs have made tremendous progress over the last few years since the early superionic solid electrolyte conductors were reported in the literature. Considering that LIBs were first invented in the 1970s and subsequently commercialized in the 1990s, followed by decades of continuous improvements and development to reach relative maturity today,²² it should come as no surprise that next-generation battery chemistries such as ASSBs would take similar pathways to enter the market and multiple levels of innovations to achieve maturity. Some of these innovations are discussed below.

Figure 1 depicts the development progression of ASSBs as a function of achievable gravimetric and volumetric energy densities for various cell configurations previously reported. The vast majority of ASSB research in the past is conducted at the half or full cell level using thick SSE separator pellets as a cell supporting structure to probe new SSE-electrode materials and its interfaces (Figures 1A and 1B).²¹ Any meaningful cell-level energy densities are only achieved when SSE thicknesses are reduced to levels ($\sim 30 \mu\text{m}$)²³ similar to separators used in LIBs (Figure 1C). Here, the ASSBs adopting graphite anode paired against lithium nickel manganese cobalt oxide (NCM) cathodes would achieve similar energy densities to the state-of-the-art LIBs ($\sim 300 \text{ Wh/kg}$). However, simply reaching parity against LIBs does not justify its competitive advantage for applications in emerging markets that required higher energy densities. From this point, several innovations in electrode and cell design unique to ASSBs have enabled breakthroughs in cell-level energy densities that exceed LIBs. One example is the adoption of high-loading composite electrodes ($>6 \text{ mAh cm}^{-2}$), typically fabricated through a dry-electrode process (Figure 1D).^{9,24} Although dry-electrode processing has also been used for LIBs,²⁵ transport limitations and liquid electrolyte wettability limit the maximum areal loadings achieved. In contrast, ASSBs utilize SSE materials directly incorporated into the cathode composite at the onset, allowing it to overcome kinetic transport limitations and deliver high capacity utilization and improved cyclability for thick

¹Department of NanoEngineering, University of California, San Diego, La Jolla, CA 92093, USA

²Pritzker School of Molecular Engineering, University of Chicago, Chicago, IL 60637, USA

*Correspondence:
dht020@eng.ucsd.edu (D.H.S.T.),
shirleymeng@uchicago.edu (Y.S.M.),
jjjang@eng.ucsd.edu (J.J.)

<https://doi.org/10.1016/j.joule.2022.07.002>

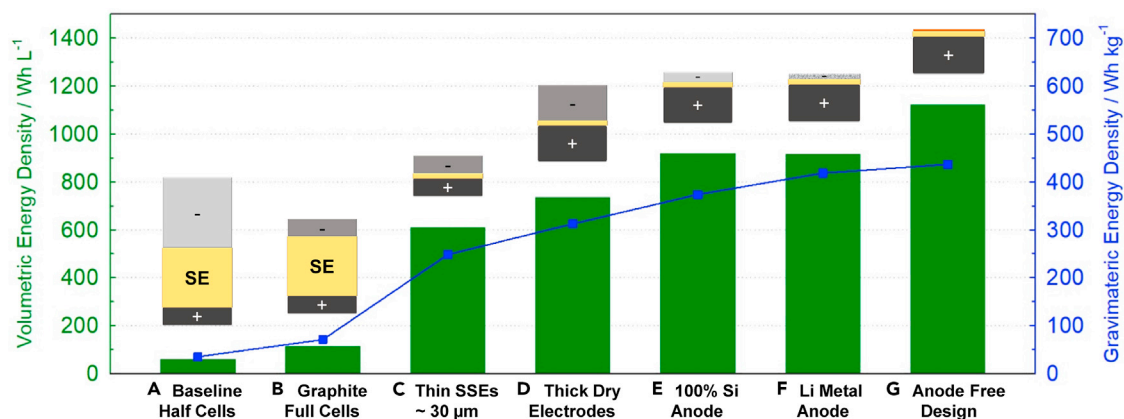


Figure 1. Calculated volumetric and gravimetric energy densities of ASSBs as a function of cell parameters

(A) Typical laboratory research half cells using Li-In anode with NP ratio ~ 20 , thick pelletized SSE separator $\sim 700 \mu\text{m}$, and 80 wt% active material NCM811 cathode composite with 200 mAh g^{-1} capacity.

(B) Use of graphite anode in full cells with NP ratio ~ 1.2 .

(C) Reducing solid electrolyte separator thickness to $\sim 30 \mu\text{m}$.

(D) Using dry-process electrodes with high loading $\sim 6 \text{ mAh cm}^{-2}$.

(E) Using a near 100% silicon anode with NP ratio ~ 1.2 .

(F) Replacing the graphite anode with Li metal anode.

(G) Adopting anode-free cell architectures. Cell parameters can be found in [Table S1](#).

electrodes. Another example of new ASSB innovations include adoption of near 100% alloy anodes such as silicon without need for carbon composites with excessive binders (Figure 1E), enabled by passivating SSEs that overcome the detrimental effects of large volume expansions and loss of Li inventory typically observed when liquid electrolytes are used.⁸ Although dense alloy materials can achieve high volumetric energy densities exceeding 900 Wh L^{-1} , high gravimetric energy densities still require use of Li metal anodes or anode-free designs (Figures 1F and 1G), which can exceed $>450 \text{ Wh kg}^{-1}$ under practical conditions as previously reported.⁹ Beyond the cell level, energy densities of ASSBs can be further improved at the module and pack level through unique stackable formats, which will be discussed in the later sections. To realize these promising innovations, ASSBs need to demonstrate viability for future production on a scale equal to or larger than LIBs.²⁶ Considering that the vast majority of research efforts are still concentrated at the laboratory scale with relatively small cell capacities ($<0.01 \text{ Ah}$), there needs to be greater focus on scaling up and development efforts at the pilot scale with more practical cell form factors ($0.1\text{--}10 \text{ Ah}$).²⁷ Thus, this perspective will discuss ASSB scalability challenges at the materials, electrode, cell stacking, and module operation level and discuss solutions to overcome prevailing prototyping challenges from the laboratory to pilot scale. As organic polymer-based ASSBs have already been extensively reported in the past since the discovery of alkali metal salt solubility in solid polymers during the 1970s,²⁸ this perspective will mainly focus on more recently studied inorganic type ASSBs, where processing methodologies are not as well understood. In addition, oxide SSEs are not considered in this ASSB perspective as the poor mechanical properties result in their requiring liquid electrolyte additives to operate.^{14,29} We place an emphasis on inorganic SSEs that show improved prospects for processing scalability without the need for liquid electrolyte additives, such as sulfide- or halide-type materials.

SOLID-STATE ELECTROLYTE SCALABILITY

Material level scalability concerns for ASSB largely pertain to the solid electrolytes. As the fundamental electrode materials (such as metallic Li or Li-alloys, transition

metal oxide cathodes) are similar to those used in LIBs, ASSB developers are able to ride along the existing material supply chain to access these electrodes in sizeable quantities. However, the same cannot be said for SSE materials, which are not yet commercially available at large quantities nor are economically competitive. To provide perspective, the Argonne National Laboratory's BatPaC manual reports commercially available liquid electrolyte (1.2 M LiPF_6 in EC:EMC) costs to be approximately $\$12.50 \text{ kg}^{-1}$, with separator costs at $\$1.10 \text{ m}^2$.³⁰ Although the costs per kg for SSEs are falling annually with increased production volumes, the same quantity of the commonly used argyrodite $\text{Li}_6\text{PS}_5\text{Cl}$ SSE today is still up to 2 orders of magnitude higher than liquid electrolytes with its corresponding separators. A significant contributing factor toward scalability is the lack of understanding in SSE synthesis, conditioning, and environmental processing protocols that limit the turnaround times and yield of high quality SSE materials needed to streamline production.

SSE synthesis

There are three primary approaches to synthesizing SSE materials reported in the literature: (1) melt quenching, (2) solution precipitation, and (3) solid-state synthesis, with solid-state synthesis being the most widely adopted method due to its simplicity and ease of scalability (Figure 2A).³¹ Although melt quenching and solution precipitation methods have yielded SSEs with high phase purity and ionic conductivities, the high melting temperatures ($>700^\circ\text{C}$) required along with need for vacuum environments and energy-intensive solvent recovery processes in solution precipitation make them unideal for large scale production of SSEs. In solid-state synthesis of sulfide- or halide-type SSEs, precursor materials are placed in a sealed jar (Figure 2A) and milled at room temperature and atmospheric pressures until reaction is complete. Although long milling and/or sintering times are typically reported in the literature ($>48 \text{ h}$ or more),^{6,32} this is unnecessary, as it possible to achieve the target phases with high ionic conductivities with short durations (1–3 h) after some process optimization. In two examples shown in Figure 2B, the sulfide $\text{Li}_6\text{PS}_5\text{Cl}$ was synthesized with 1 h of ball milling and heat treatment, after which, saturation is achieved, and any extra milling time is deemed excessive and unnecessary. Likewise, the halide Li_2ZrCl_4 reached a maximum ionic conductivity near 1 mS cm^{-1} under ball milling of 3 h without heat treatment, potentially reducing resources needed to scale production of such SSE materials.

SSE conditioning

Although SSEs can be directly used after synthesis, post-synthesis conditioning steps are crucial to reduce particle sizes and size distribution. To achieve this, the SSEs can be directly homogenized in the same synthesis reaction vessel at lower milling rates. Addition of non-polar solvents (for wet milling) such as xylene or toluene has also been found to aid in reducing particle size distribution before being removed via vacuum drying (Figure 2C left).³³ Figure 2D summarizes the SSE particle sizes and morphologies of dry versus wet milling methods. Although sub-micron SSE particles can be attained with dry milling, wet milling remains to be most effective in achieving a more homogeneous distribution. Alternatively, automated sieving tools (Figure 2C right) can be utilized to filter large particles if solvent processing is to be avoided. The large particles collected can then be milled and sieved repeatedly to maximize yield. The cell performance effects of using smaller particle-sized SSEs are shown in Figure 2E, where higher capacity utilization and improved rate capabilities can be achieved. However, it is noted that excessive SSE conditioning through ball milling may reduce the ionic conductivity of the material as previously reported.³³

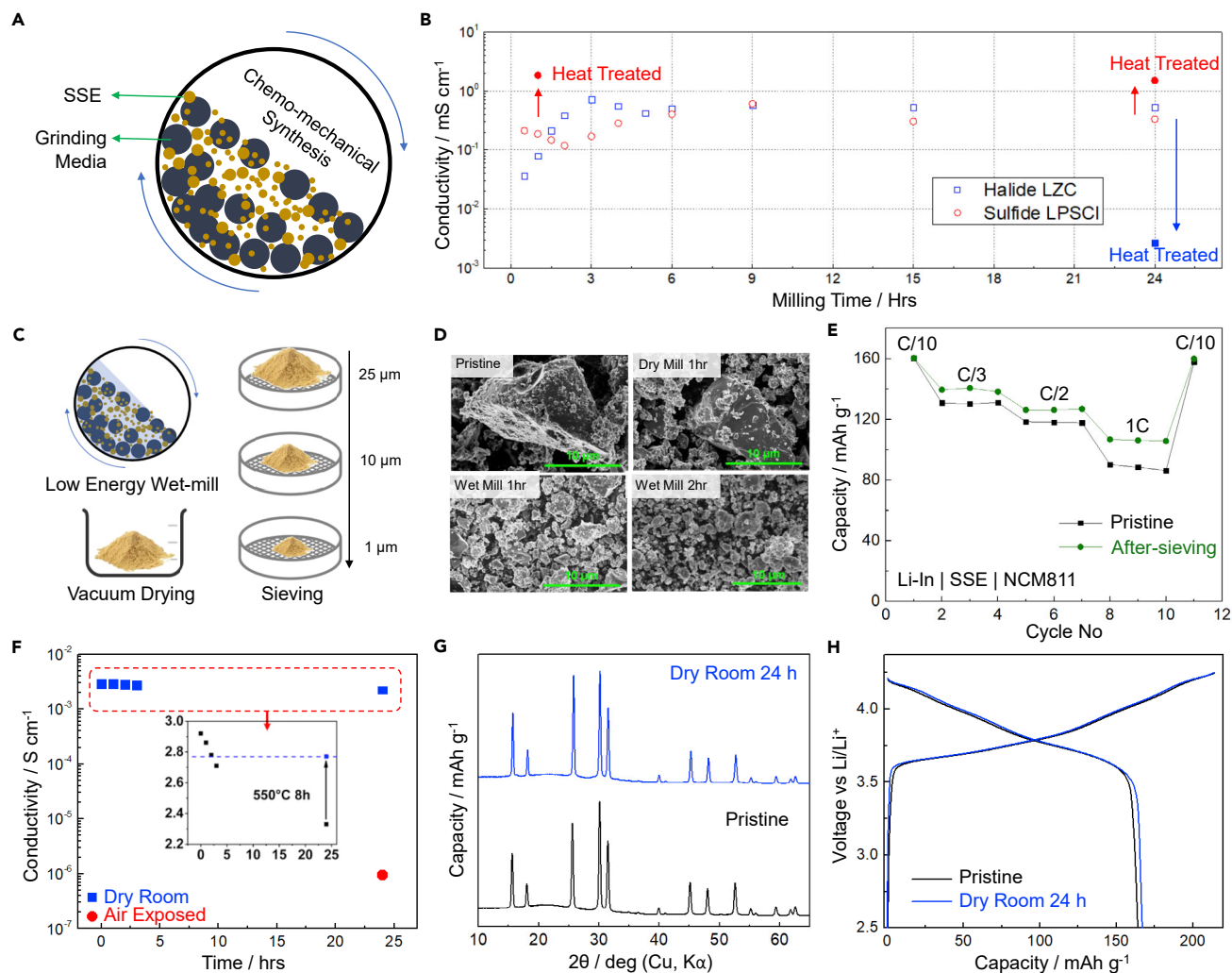


Figure 2. Solid-state electrolyte material scalability

(A) Schematic of single-step room temperature dry chemo-mechanical synthesis.

(B) Ionic conductivities of halide Li₂ZrCl₆ (LZC) and sulfide Li₆PS₅Cl (LPSCI) solid electrolyte after ball milling and heat treatment. Showing that long synthesis durations commonly used can be avoided.

(C) Post-synthesis conditioning steps to reduce particle size.

(D–H) (D) SEM images of SSE particles after post-synthesis treatment³³ and (E) rate performance comparisons. Dry-room stability of sulfide SSEs with (F) ionic conductivity, (G) X-ray diffraction and (H) electrochemical cycling voltage curves.³⁴

Dry-room stability

Similar to liquid electrolytes, solid electrolytes need to be handled in moisture-free environments. When exposed to H₂O, sulfide- and halide-type SSEs undergo a combination of hydrolysis and hydration, irreversibly releasing H₂S or HCl toxic gases in the process, making them intrinsically incompatible with ambient environments.^{34,35} However, certain SSEs have been found to be highly stable in dry rooms (~−40°C dew point), under conditions not too different from those used in LIB manufacturing, making them safe to handle without significant risks of H₂S or HCl gas exposure. After 24 h of exposure in such conditions, the sulfide Li₆PS₅Cl was reported to retain most of its ionic conductivity (Figure 2F) as well as bulk structure (Figure 2G). Electrochemically, SSEs exposed under dry-room conditions exhibited virtually identical cell performance when compared with the pristine state (Figure 2H), indicating that inert (Ar or N₂) environments currently used in most laboratories are not necessary if

dry-room conditions are available. Although such extensive studies also need to be conducted for other SSE materials, there is little evidence indicating severe degradation of SSE function against moisture-free environments. Thus, it is likely that future scalable production of SSEs can be conducted in the dry room.

ELECTRODE AND SEPARATOR PROCESSING

Beyond synthesis, scalability challenges of SSEs are associated with its incorporation into cathode electrode composites. Early attempts to demonstrate ASSBs in pouch-type-cell form factors involved slurry-based casting of both cathode composites and SSEs with non-polar solvents.^{36,37} However, the inherent limitations of slurry-based processes limited the maximum areal loadings achieved due to the vast differences in physical properties of SSEs, cathodes, and carbon additives suspended within the slurry, making it challenging to maintain homogeneity and mechanical integrity in thick electrodes without excessive binder usage. To overcome this, recent trends in thick electrode processability have made significant inroads in composite electrodes for ASSBs, achieving areal loadings exceeding $>10 \text{ mAh cm}^{-2}$ in some cases,^{8,38} significantly higher than that achievable in LIB casting methods. Moreover, high-loading dry electrodes can be fabricated using minimal amounts of binder, with past reports demonstrating free-standing electrode composites made with just 0.1 wt% polytetrafluoroethylene (PTFE) binder.³⁹ The absence of solvent-drying processes also reduces energy consumption requirements, as nearly half (~48%) of energy costs in LIB production comes from drying steps, potentially improving scalability and costs of ASSB fabrication.⁴⁰

Dry-electrode fabrication

In principle, dry-electrode fabrication involves two main components: mixing and shearing.²⁴ In mixing, the cathode electrode composites are homogeneously dispersed with PTFE binders using mild mixing conditions to prevent agglomeration of particles. [Figure 3A](#) illustrates an example of dry-composite mixing using a centrifugal mixer, which can be scaled to accommodate larger batch sizes when larger mixing vessels are used. Subsequently, the homogeneous powders will be extruded using sequential rolling presses until the target thicknesses are achieved ([Figure 3B](#)), using tools similar those used to calendar slurry-casted cathode electrodes in LIBs. This approach applies to dry processing of SSE separator layers as well. The eventual form factors and throughput of dry electrodes fabricated would depend on the dimensions of hot rollers available as well as the speed of the rollers. The scalable nature of dry-electrode processability for ASSBs are highly dependent on the mechanical properties of the SSEs chosen ([Figure 3C](#)).⁴¹ As dry electrodes are fabricated at near room temperature conditions, it is vital that SSE materials used are malleable and can achieve sufficient deformability for dense packing without need for high temperature sintering that may induce thermal decomposition of the binders used. Examples of such materials include sulfide- and halide-type SSEs that are typically densified at room temperature. However, it is noted that large scale processing tools for dry-electrode extrusion are not yet readily available. This, coupled with the need for such tools to process SSEs in dry-room conditions, make it one of the major challenges for ASSB dry-electrode scalability.

Solvent-free cell prototyping

In previous studies on slurry-based casting, the dissolved or dispersed binders are precipitated in film-like structures around each solid electrolyte particle ([Figure 3D](#)), which may increase impedance due to increased tortuosity of Li^+ diffusion pathways, resulting in significant ionic conductivity losses (~50%) compared with the pristine SSE material.^{37,43} On the other hand, the dry-process shearing steps result in a

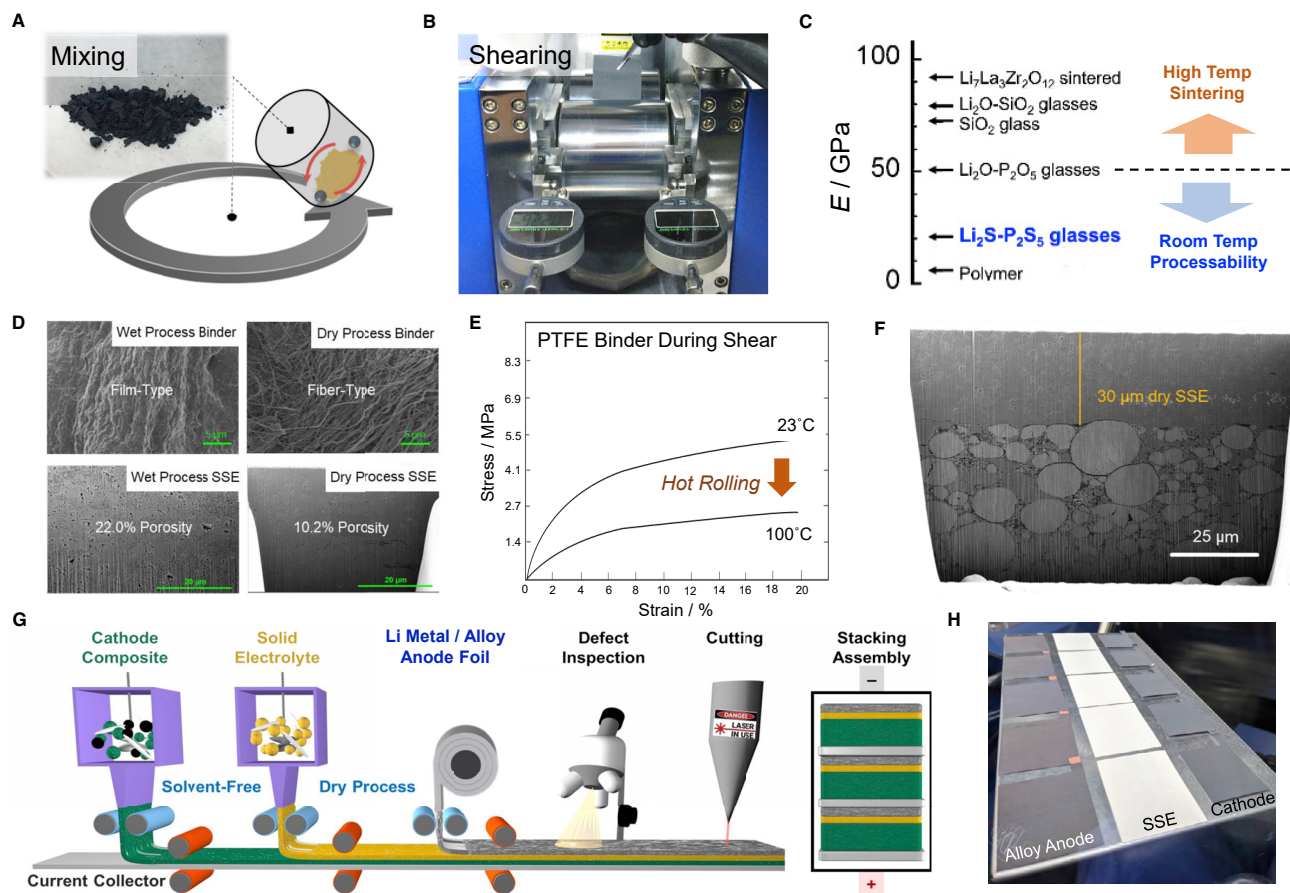


Figure 3. Composite electrodes and separator scalable fabrication

- (A) Schematic of planetary centrifugal mixer used to disperse PTFE binders, active material, solid electrolytes, and carbon. Inset shows digital image of mixed composite.
 (B) Digital image of dry-electrode shearing process derived from mixed powders.
 (C) Mechanical properties of various solid electrolyte materials.⁴¹
 (D) SEM images of binders and solid electrolyte composites fabricated using wet versus dry processing.
 (E) Stress-strain profile of PTFE binder used in dry processing,⁴² toughness reduction effects of hot rolling.
 (F) FIB-SEM cross section image of dry SSE separator laminated on a dry cathode composite.
 (G and H) (G) Schematic dry ASSB manufacturing and (H) digital images of individual layers.

fiber-like morphology of binders weaving through SSE particles instead of covering their surfaces entirely. This morphology, combined with the reduced binder wt% required to produce free-standing films allow minimal losses to ionic conductivity and Li⁺ diffusion pathways. Additionally, the continuous shearing steps of dry processing allows much denser packing of SSE particles compared with particles within slurry suspensions, resulting in significantly reduced porosities after calendaring (Figure 3D). Although dry processing can be conducted at room temperature, the amount of uniaxial line-force (and therefore rolling speed and number of rolling steps) can be dramatically reduced when elevated temperatures are used. As shown in Figure 3E, the amount of stress applied on the same PTFE binder under the same degree of strain at room temperature can be halved when sheared at 100°C.⁴² Therefore, to increase throughput in efforts to facilitate scalability of dry processing, heated rollers can be used to minimize total applied stresses required. With sufficient shearing, the thickness of free-standing films can be controlled with micron-scale precision. Figure 3F shows the cross section scanning electron microscopy

(SEM) image of a dry SSE separator of 30 μm thickness laminated to a dry NCM811 cathode electrode, showing good interfacial contact between the layers with low overall porosity. With innovations in dry processing of SSE separators and cathode composites, as well as adoption of Li metal or near 100% Li-alloy anodes, it is conceivable that ASSB layers can be assembled without use of solvents (Figure 3G). An example of repeat units of μSi alloy anodes, SSE separators, and cathode composite electrodes made at the laboratory scale is shown in Figure 3H. The next section will discuss how these layers can be stacked to form multi-layer ASSBs.

CELL ASSEMBLY AND CONFIGURATIONS

Stacking strategies

For ASSB scalable prototyping to be successful, it is imperative for processes to mimic LIB compatible manufacturing tools. This reduces the need to re-invent or retrofit new machinery to support fabrication steps that may not yet exist. ASSBs need to be designed for stacking and assembly using commercially available tools with minimal modifications. In LIBs, cell assembly methods include individual sheet stacking, Z-folding, and winding for either prismatic or cylindrical cell form factors.⁴⁴ Considering that ASSBs will likely adopt pouch-type form factors that facilitate application of stack pressure, individual sheet stack or Z-folding can be explored. Individual sheet stacking for single to bi-layer pouch-type cells have already been previously reported.^{9,45} However, such methods face potential misalignment issues that can induce cell short, often requiring large space tolerances (~ 0.5 cm) along the edges to act as a buffer. To mitigate this, Z-folding can also be used to eliminate risks of anode-cathode direct contact, as seen in Figure 4A. Here, an extended free-standing SSE separator is folded to allow the anode and cathode electrode layers to be slotted into alternating folds, which can be conducted with automation using commercially available z stacking tools. The mechanical strength of the SSE films also needs to be considered when applied to commercial z stacking tools, where the line tension would need to be optimized to tune the tensile forces applied to the SSE film. Alternatively, mechanically compliant polymer-supported SSE films can be used to improve mechanical strength as previously reported.^{46,47}

Stacking and densification

ASSBs also offer the unique option to adopt series (bi-polar) stacking designs, where LIBs mainly adopt parallel (bi-layer) stacking. Stacking layers in series reduces use of inactive material components such as tabs and internal wiring (Figure 4B), potentially increasing the overall packing density and module level energy density. Furthermore, stacking in series achieves a higher overall voltage per cell (Figure 4C), as seen in an example using the $\mu\text{Si}|\text{SSE}|\text{NCM811}$ cell configuration, potentially reducing voltage-ramping requirements in high-voltage devices. However, it should be noted that meaningful comparisons and demonstrations of bi-polar stacking benefits are not well established yet. Recognizing that potential energy density and performance gains of bi-polar configurations are mainly realized at the module to pack level, both parallel and series stacking of ASSBs will likely still be explored at the cell level simultaneously, with parallel stacking being the more established method used for current prototypes.

After stacking, the cell layers need to be densified to reduce porosity as well as increase physical contact between the electrode and SSE interfaces. This is typically done using three primary methods, continuous line pressing, uniaxial areal pressing, and isostatic pressing (Figure 4D). Line pressing (or calendaring) remains to be the most used method to reduce porosities in LIBs, mainly due to its high throughput and ease of scalability.⁴⁸ Unfortunately, considering the high fabrication pressures

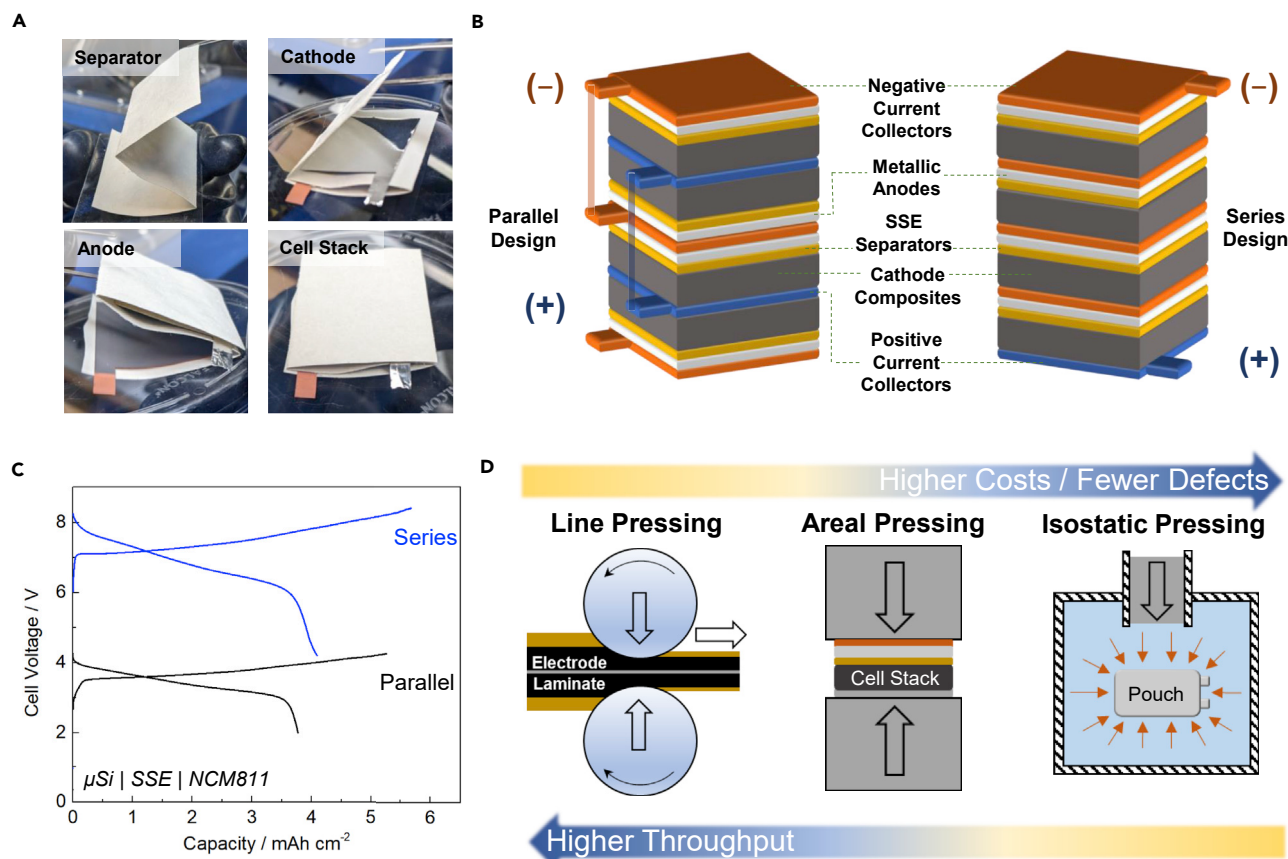


Figure 4. Cell assembly and configurations

(A) Z stacking example using sulfide $\text{Li}_6\text{PS}_5\text{Cl}$ solid electrolyte sandwiched between anode and cathode electrode layers. Digital images are displayed for reference.

(B) Schematic of parallel- (bi-layer) versus series- (bi-polar) stacking design.

(C) Reference voltage profile of parallel- versus series-stacked ASSB design.

(D) Schematic of three major strategies to achieve densification of electrolyte/electrode layers within pouch-type cells.

(exceeding 300 MPa) needed to densify ASSBs, the large amounts of force applied often result in drastic inhomogeneities in the SSE and electrode layers and at times induce mechanical cracking of the sheets. Thus, uniaxial pressing is still the dominant approach used to densify ASSBs, which can be done before or after pouch sealing. Although uniaxial densification works well at the laboratory scale, its major shortcomings include the ability to densify larger form-factor pouch cells, as the ton-force required linearly increases with cell area, requiring proportionately larger hydraulic presses to densify larger ASSB pouch cells. To overcome this, isostatic pressing is considered, which have been shown to achieve highly dense electrode morphologies and can accommodate ASSBs of any size, limited only by the dimensions of the isostatic pressure vessel.⁹ However, high upfront costs as well as the impractical sizes of isostatic pressing machines may limit their usage in small laboratory settings.

CELL TO MODULE CONSIDERATIONS

ASSB operating conditions

Unlike conventional LIBs, ASSBs require significant amounts of stack pressure in order to operate. Interestingly, there is no consensus within the field on the precise stack pressure value needed. Past studies have reported stack pressures ranging

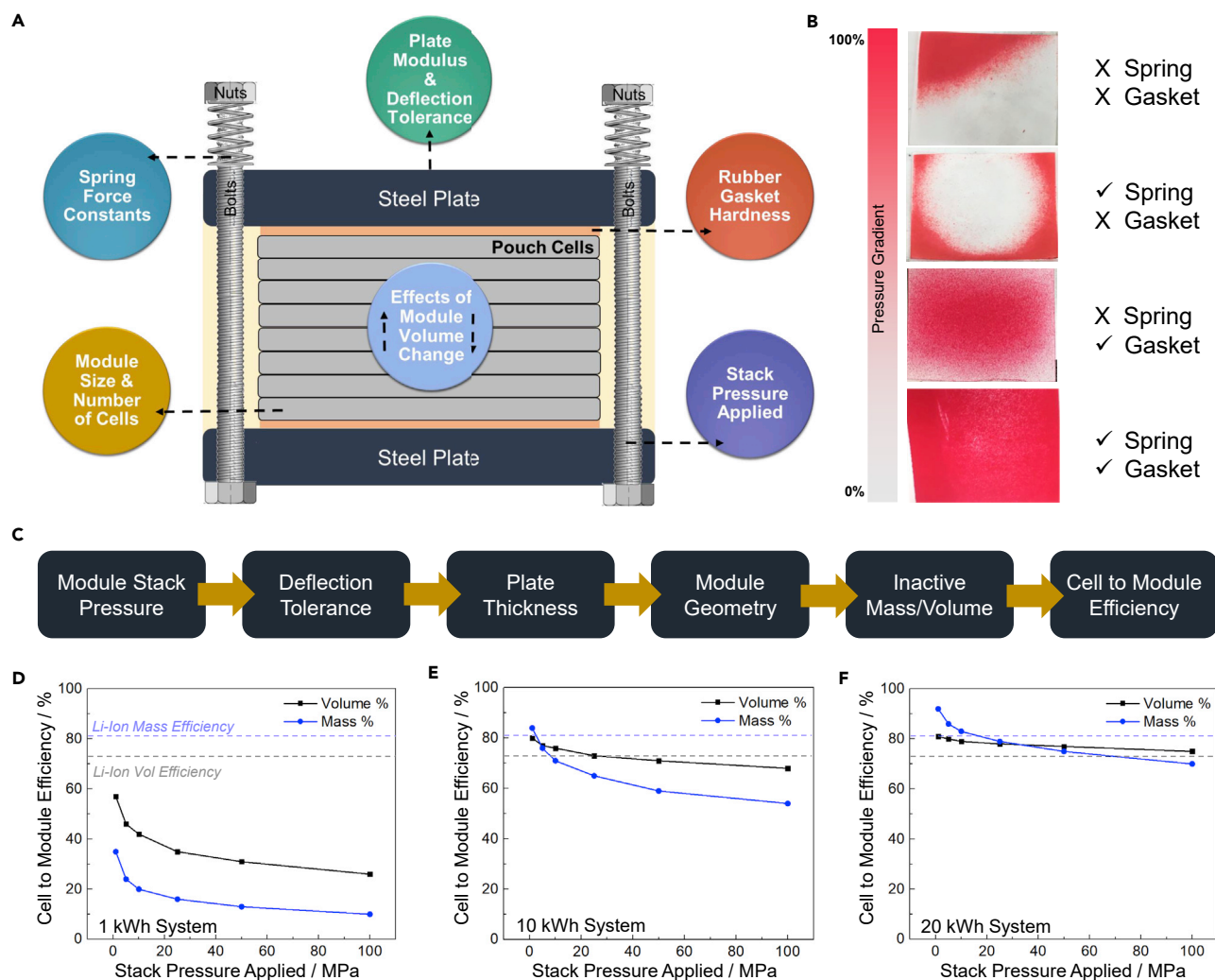


Figure 5. Cell to module operational considerations

(A) Schematic of typical ASSB module assembly under stack pressure. Vital consideration factors are shown.

(B) Importance of applying uniform stack pressure with the use of springs and gaskets and pressure paper feedback tool.

(C–F) (C) Workflow to model cell to module conversion efficiencies. Cell to module conversion efficiencies versus stack pressure based on a system size of (D) 1 kWh, (E) 10 kWh, and (F) 20 kWh. Li-ion cell to module conversion efficiencies by mass and volume are displayed for reference.

from 3 to 7 MPa for Li metal-based ASSBs^{49,50} to as high as 50–200 MPa for Li-alloy based ASSBs.^{6,8} However, nearly all values are reported based on small area pellet type cell designs ($\sim 1 \text{ cm}^2$), where single point loads are typically applied and monitored. In multi-layer and multi-pouch cell stacks, application of stack pressure, its 2D areal homogeneity, as well as the ability to maintain a constant pressure throughout cell cycling make it far more sophisticated to design cell to module structures to house ASSBs. Figure 5A below depicts a typical ASSB pouch cell stack sandwiched between two metal plates held by bolts along the edges to apply stack pressure. Considerations for the housing designs are: (1) module dimensions and number of cells, (2) supporting spring force constants, (3) metal plate modulus and deflection tolerance allowed, (4) shore hardness of rubber gaskets, (5) stack pressure applied, and (6) degree of volume change experienced in the z axis. Due to the lack of any published studies on ASSB housing designs, there is a limited understanding on how these parameters are correlated and how they impact overall cell performance

within the stack. There is an urgent need for a shift in focus beyond materials to electrodes level research, toward cell and module-stacking design considerations that remain to be one of the biggest challenges limiting scale-up of ASSB prototyping. Unlike LIB research grade coin cells, that have widely accepted standardized form factors and internal structure, most ASSB cell housings are custom made, and details of its designs are seldom reported, creating large disparities in findings across different research groups. For instance, despite recent efforts to evaluate stack pressure effects on performance metrics such as critical current density and capacity retention on ASSBs, little to no attention is given to the homogeneity of stack pressures applied, which can have drastic consequences on the cell, possibly explaining the wide ranges of stack pressures used in the literature. To illustrate this, effects of four different pouch-housing configurations are shown in [Figure 5B](#) using pressure sensitive films.

In the absence of springs and gaskets, pressure distribution throughout the pouch cell's area is observed to be highly inhomogeneous ([Figure 5B top](#)), likely due to a combination of uneven loads applied on the bolts as well as inherent roughness of the metal plates used. If either springs or gaskets are used, pressure is better distributed either to the edges in the cases where only springs are used or concentrated in the center where the gaskets are most highly compressed ([Figure 5B middle](#)). Finally, stack pressure is found to be the most uniform when a combination of springs and gaskets are used ([Figure 5B bottom](#)). It is important to note that even within the subset of the 6 considerations discussed above, there are numerous parameters to explore and optimize, making it impractical to investigate via traditional trial and error methods. To this end, if a sizeable dataset can be generated, such parameters can then be modeled more effectively using machine learning tools that can provide guidelines to design an ideal ASSB housing structure.⁵¹

Cell-to-module conversion efficiency

Besides its influence on cell performance, stack pressures can also directly influence module designs that in turn, significantly affect cell-to-module conversion efficiencies attainable. To provide a frame of reference, mean cell-to-module conversion efficiencies for LIB pouch-type cells are reportedly 73% and 82% for volumetric and gravimetric efficiencies, respectively,⁵² with most of the inactive mass/volume coming from module housing and supporting structures. To model the conversion efficiencies of ASSBs based on stack pressure, several assumptions with regards to module design were made based on a edge supported rectangular flat plate with uniform load applied design⁵³: (1) plate deflection tolerance of $L/500$ (where L is plate span) is chosen, a more conservative value than $L/240$ and $L/360$ recommended by ACI code beam deflection standards, (2) carbon steel plates are chosen with a bulk modulus of 200 GPa, and (3) inactive mass/volume contributions only from the supporting metal structures. It is noted that the calculations seek to study the effects of stack pressure and system size on the ASSB cell-to-module conversion efficiencies and not as a comparison against LIB systems. The model workflow based on these assumptions is illustrated in [Figure 5C](#), and details of the calculations can be found in [Figure S1](#). ASSB cell-to-module conversion efficiencies are calculated for various stack pressures applied (from 1 to 100 MPa) and compared across different system sizes. For a relatively small system size of 1 kWh, the ASSB module displays poor conversion efficiency both by mass and volume even at relatively low pressures ([Figure 5D](#)), indicating that ASSBs are unlikely to be competitive for smaller device applications. However, as the system size is increased, the active to inactive material ratio of the ASSB module increases dramatically, allowing cell-to-module conversion efficiencies of ASSBs to exceed those of LIBs especially at stack

Table 1. Summary of the scale, methods, focus, and barriers of research and development at different levels are summarized below

	Laboratory research	Pilot prototyping	Production scale
Cell size	0.001–1 Ah	0.1–10 Ah	>10 Ah cells/kWh packs
Methods	manual—gloveboxes environments	semi-automated—gloveboxes and dry room	fully automated—large footprint dry labs
Focus	material discovery and screening	chemistry and design validation	cost and throughput optimization
Barriers	access to resources and tools	scalability and new materials supply chain	defect elimination for quality control

pressures of 5 MPa or less (Figures 5E and 5F). Consequently, this would have an effect of increased costs for downstream system integrators, who will need additional resources to apply and maintain stack pressures at the system level. From this model, it is observed that conversion efficiencies losses by mass are significantly more sensitive to increases in stack pressures compared with by volume. This suggests that ASSBs can offer a competitive advantage in applications where volumetric energy densities are of greater importance, such as in stationary storage applications. In mobility applications where gravimetric energy density is crucial, stack pressures need to be kept as low as possible to minimize conversion efficiency losses.

ACCELERATING SCALE-UP THROUGH PARTNERSHIPS

Compared with the vast number of impactful laboratory-scale discoveries reported in the ASSB literature, few of these breakthroughs have yet to directly translate into commercialized products. University-led laboratory-scale research, typically conducted by academic scientists focusing on material discovery and screening, utilizes small capacity type testing cells, which may not provide sufficient data or practical validation required for industrial evaluation where throughput and defect elimination are concerned (Table 1). As such, universities often lack the resources to extrapolate the electrochemical and physicochemical properties of prototypes relevant for the industry. Additionally, the current academic evaluation system provides little incentive for university scientists to bridge this gap, forming a development bottleneck between lab and market that is filled haphazardly by start-up companies. Such start-up companies situated in the middle of laboratory discoveries are often spun-out by their founders, and large corporations adopt a “wait and see” approach, mainly participating when a certain levels of technology-readiness levels are reached. Although successful discoveries in the laboratory are widely publicized in academic journals, start-up companies prefer to protect successful practices, making information availability for pilot-scale prototyping limited. This behavior is characterized by the “free-rider” problem, where despite widespread benefits to the entire community if such crucial information is shared, the companies that invested heavily in its development would have little incentive to share best practices and data collected. To make matters worse, most start-ups encounter multiple valleys-of-deaths during their growth (Figure 6), often due to reasons unrelated to the technology itself, resulting in loss of valuable knowledge gained through their research and development efforts. Conversely, academic scientists never shy away from an opportunity to publish or publicly discuss their findings, due to inherent non-financial benefits as part of the academic evaluation system. As such, the field is faced with an inefficiency gap that must be bridged by a 3rd party instead. Ideally, this is done by public institutions that have non-economic or other national interests in the technology’s success, such as national laboratories equipped with resources to perform research at the pilot scale. By investing in mid-level testing laboratories within accessible national laboratories, with the overarching purpose of testing and validating promising discoveries from the laboratory in scales more relevant to industry but yet of scientific interest to academic researchers, it provides an effective balance of the needs of both academia and industry (Figure 6).



Figure 6. Accelerating scale-up of new battery technologies through university, national laboratory, and industry partnerships

Importance of incentivizing transfer of knowledge and know-how through private-public funded collaborative efforts, avoiding the common death valleys of risky start-up companies, where vital intellectual property and development know-how are lost.

A successful past example of such an approach is seen through the Battery500 consortium led by the Pacific Northwestern National Laboratory (PNNL).⁵⁴ With key focus areas on enabling high energy density Li metal anodes and conversion based sulfur cathodes for LIBs, efforts were focused on demonstrating innovations with Ah-sized pouch cells. This was achieved through collaborations between participating members of the consortium that included scientists from universities as well as engineers from major corporations. Being a publicly funded program, all findings were publicly shared through periodic reports for the benefit of the entire energy storage research community. Such scientific publications that include performance and manufacturing demonstration on the pilot scale with larger cell capacities also raises the academic credibility of scientists who conduct the research. As an example, this was demonstrated when Samsung released a complete dataset of their anode-free ASSB pouch cell manufactured entirely in a dry room, which made a large enough impact on the energy storage community to quell many misconceptions about ASSBs manufacturability in LIB compatible environments.⁹ Such capabilities, if available and accessible, would also instill confidence within public funding agencies during evaluation of proposed concepts and ideas from start-up companies, raising the overall success rates of projects funded, and potentially shave years off pathways for technology commercialization. Development of ASSBs is on the cusp of widespread market penetration. The past two decades have propelled major breakthroughs in fundamental understanding, interfacial stabilization, and electrode to cell-level design. Beyond this phase, focus now needs to be concentrated on process scalability and pilot-scale prototyping, for scalability itself is a form of innovation that should not be overlooked.

SUPPLEMENTAL INFORMATION

Supplemental information can be found online at <https://doi.org/10.1016/j.joule.2022.07.002>.

ACKNOWLEDGMENTS

This work was funded by the LG Energy Solution through the Frontier Research Laboratory (FRL) Program and the National Science Foundation—Partnerships for Innovation (NSF-PFI) grant no. 2044465. The authors acknowledge the support of UNIGRID Battery, a UCSD spin-out company for the ASSB prototyping capabilities. The authors would also like to acknowledge the UCSD Crystallography Facility. This work was performed in part at the San Diego Nanotechnology Infrastructure (SDNI) of UCSD, a member of the National Nanotechnology Coordinated Infrastructure, which is supported by the National Science Foundation (grant ECCS-1542148), along with the use of facilities and instrumentation supported by NSF through the UC San Diego Materials Research Science and Engineering Center (UCSD MRSEC), grant #DMR-201192.

DECLARATION OF INTERESTS

The authors declare no competing interests.

REFERENCES

1. Wang, Y., Richards, W.D., Ong, S.P., Miara, L.J., Kim, J.C., Mo, Y., and Ceder, G. (2015). Design principles for solid-state lithium superionic conductors. *Nat. Mater.* **14**, 1026–1031.
2. Tan, D.H.S., Banerjee, A., Chen, Z., and Meng, Y.S. (2020). From nanoscale interface characterization to sustainable energy storage using all-solid-state batteries. *Nat. Nanotechnol.* **15**, 170–180.
3. Xu, L., Li, J., Deng, W., Shuai, H., Li, S., Xu, Z., Li, J., Hou, H., Peng, H., Zou, G., and Ji, X. (2021). Garnet solid electrolyte for advanced all-solid-state Li batteries. *Adv. Energy Mater.* **11**, 2000648.
4. Chen, S., Xie, D., Liu, G., Mwizerwa, J.P., Zhang, Q., Zhao, Y., Xu, X., and Yao, X. (2018). Sulfide solid electrolytes for all-solid-state lithium batteries: structure, conductivity, stability and application. *Energy Storage Mater.* **14**, 58–74.
5. Pang, Y., Liu, Y., Yang, J., Zheng, S., and Wang, C. (2022). Hydrides for solid-state batteries: a review. *Mater. Today Nano* **18**, 100194. <https://doi.org/10.1016/j.mtnano.2022.100194>.
6. Zhou, L., Zuo, T., Kwok, C.Y., Kim, S.Y., Assoud, A., Zhang, Q., Janek, J., and Nazar, L.F. (2022). High areal capacity, long cycle life 4 V ceramic all-solid-state Li-ion batteries enabled by chloride solid electrolytes. *Nat. Energy* **7**, 83–93.
7. Liang, F., Sun, Y., Yuan, Y., Huang, J., Hou, M., and Lu, J. (2021). Designing inorganic electrolytes for solid-state Li-ion batteries: a perspective of LGPS and garnet. *Mater. Today* **50**, 418–441.
8. Tan, D.H.S., Chen, Y.T., Yang, H., Bao, W., Sreenarayanan, B., Doux, J.M., Li, W., Lu, B., Ham, S.Y., Sayahpour, B., et al. (2021). Carbon-free high-loading silicon anodes enabled by sulfide solid electrolytes. *Science* **373**, 1494–1499.
9. Lee, Y.-G., Fujiki, S., Jung, C., Suzuki, N., Yashiro, N., Omoda, R., Ko, D.-S., Shiratsuchi, T., Sugimoto, T., Ryu, S., et al. (2020). High-energy long-cycling all-solid-state lithium metal batteries enabled by silver-carbon composite anodes. *Nat. Energy*.
10. Doerrer, C., Capone, I., Narayanan, S., Liu, J., Grovenor, C.R.M., Pasta, M., and Grant, P.S. (2021). High energy density single-crystal NMC/Li₆PS₅Cl cathodes for all-solid-state lithium-metal batteries. *ACS Appl. Mater. Interfaces* **13**, 37809–37815.
11. Banerjee, A., Wang, X., Fang, C., Wu, E.A., and Meng, Y.S. (2020). Interfaces and interphases in all-solid-state batteries with inorganic solid electrolytes. *Chem. Rev.* **120**, 6878–6933.
12. Liang, J., Luo, J., Sun, Q., Yang, X., Li, R., and Sun, X. (2019). Recent progress on solid-state hybrid electrolytes for solid-state lithium batteries. *Energy Storage Mater.* **21**, 308–334.
13. Verdusco, J.C., Vergados, J.N., Strachan, A., and Marinero, E.E. (2021). Hybrid polymer-garnet materials for all-solid-state energy storage devices. *ACS Omega* **6**, 15551–15558.
14. Hitz, G.T., McOwen, D.W., Zhang, L., Ma, Z., Fu, Z., Wen, Y., Gong, Y., Dai, J., Hamann, T.R., Hu, L., and Wachsman, E.D. (2019). High-rate lithium cycling in a scalable trilayer Li-garnet-electrolyte architecture. *Mater. Today* **22**, 50–57.
15. Zhang, X., Liu, T., Zhang, S., Huang, X., Xu, B., Lin, Y., Xu, B., Li, L., Nan, C.W., and Shen, Y. (2017). Synergistic coupling between Li_{6.75}La₃Zr_{1.75}Ta_{0.25}O₁₂ and poly(vinylidene fluoride) induces high ionic conductivity, mechanical strength, and thermal stability of solid composite electrolytes. *J. Am. Chem. Soc.* **139**, 13779–13785.
16. Wang, C., Sun, Q., Liu, Y., Zhao, Y., Li, X., Lin, X., Banis, M.N., Li, M., Li, W., Adair, K.R., et al. (2018). Boosting the performance of lithium batteries with solid-liquid hybrid electrolytes: interfacial properties and effects of liquid electrolytes. *Nano Energy* **48**, 35–43.
17. Yi, E., Shen, H., Heywood, S., Alvarado, J., Parkinson, D.Y., Chen, G., Sofie, S.W., and Doeff, M.M. (2020). All-solid-state batteries using rationally designed garnet electrolyte frameworks. *ACS Appl. Energy Mater.* **3**, 170–175.
18. Luo, W., Gong, Y., Zhu, Y., Li, Y., Yao, Y., Zhang, Y., Fu, K.K., Pastel, G., Lin, C.F., Mo, Y., et al. (2017). Reducing interfacial resistance between garnet-structured solid-state electrolyte and Li-metal anode by a germanium layer. *Adv. Mater.* **29**, 1606042.
19. Shao, Y., Wang, H., Gong, Z., Wang, D., Zheng, B., Zhu, J., Lu, Y., Hu, Y., Guo, X., Li, H., et al. (2018). Drawing a soft interface: an effective interfacial modification strategy for garnet-type solid-state Li batteries. *ACS Energy Lett.* **3**, 1212–1218.
20. Albertus, P., Anandan, V., Ban, C., Balsara, N., Belharouk, I., Buettner-Garrett, J., Chen, Z., Daniel, C., Doeff, M., Dudney, N.J., et al. (2021). Challenges for and pathways toward Li-metal-based all-solid-state batteries. *ACS Energy Lett.* **1399**–1404.
21. Randau, S., Weber, D.A., Kötz, O., Koerver, R., Braun, P., Weber, A., Ivers-Tiffée, E., Adermann, T., Kulisch, J., Zeier, W.G., et al. (2020). Benchmarking the performance of all-solid-state lithium batteries. *Nat. Energy* **5**, 259–270.
22. Li, M., Lu, J., Chen, Z., and Amine, K. (2018). 30 years of lithium-ion batteries. *Adv. Mater.* **30**, e1800561.
23. Wu, J., Yuan, L., Zhang, W., Li, Z., Xie, X., and Huang, Y. (2021). Reducing the thickness of solid-state electrolyte membranes for high-energy lithium batteries. *Energy Environ. Sci.* **14**, 12–36.
24. Lu, Y., Zhao, C., Yuan, H., Hu, J., Huang, J., and Zhang, Q. (2022). Dry electrode technology, the rising star in solid-state battery industrialization. *Matter* **5**, 876–898.
25. Ludwig, B., Zheng, Z., Shou, W., Wang, Y., and Pan, H. (2016). Solvent-free manufacturing of electrodes for lithium-ion batteries. *Sci. Rep.* **6**, 23150.
26. Lee, J., Lee, T., Char, K., Kim, K.J., and Choi, J.W. (2021). Issues and advances in scaling up sulfide-based all-solid-state batteries. *Acc. Chem. Res.* **54**, 3390–3402.
27. Xu, L., Lu, Y., Zhao, C., Yuan, H., Zhu, G., Hou, L., Zhang, Q., and Huang, J. (2021). Toward the scale-up of solid-state lithium metal batteries: the gaps between lab-level cells and practical large-format batteries. *Adv. Energy Mater.* **11**, 2002360.
28. Fenton, D.E., Parker, J.M., and Wright, P.V. (1973). Complexes of alkali metal ions with poly(ethylene oxide). *Polymer* **14**, 5898.
29. Song, X., Wang, C., Chen, J., Xin, S., Yuan, D., Wang, Y., Dong, K., Yang, L., Wang, G., Zhang, H., and Zhang, S. (2021). Unraveling the synergistic coupling mechanism of Li⁺ transport in an “ionogel-in-ceramic” hybrid solid electrolyte for rechargeable lithium metal battery. *Adv. Funct. Mater.* **32**, 2108706.
30. Nelson, P.A., Shabbir, A., Gallagher, K.G., and Dees, D.W. (2019). Modeling the performance and cost of lithium-ion batteries for electric-drive vehicles (Argonne National Laboratory—Electrochemical Communications Energy Storage Department Chemical Sciences and Engineering Division).
31. Kudu, Ö.U., Famprikis, T., Fleutot, B., Braidia, M., Le Mercier, T., Islam, M.S., and Masquelier, C. (2018). A review of structural properties and synthesis methods of solid electrolyte materials in the Li₂S–P₂S₅ binary system. *J. Power Sources* **407**, 31–43.
32. Ji, X., Hou, S., Wang, P., He, X., Piao, N., Chen, J., Fan, X., and Wang, C. (2020). Solid-state electrolyte design for lithium dendrite suppression. *Adv. Mater.* **32**, e2002741.
33. Chen, Y.-T., Duquesnoy, M., Tan, D.H.S., Doux, J., Yang, H., Deysher, G., Ridley, P., Franco, A.A., Meng, Y.S., and Chen, Z. (2021). Fabrication of high-quality thin solid-state electrolyte films assisted by machine learning. *ACS Energy Lett.* **1639**–1648.
34. Chen, Y.-T., Marple, M.A.T., Tan, D.H.S., Ham, S., Sayahpour, B., Li, W., Yang, H., Lee, J.B., Hah, H.J., Wu, E.A., et al. (2022). Investigating dry room compatibility of sulfide solid-state electrolytes for scalable manufacturing. *J. Mater. Chem. A* **10**, 7155–7164.
35. Li, W., Liang, J., Li, M., Adair, K.R., Li, X., Hu, Y., Xiao, Q., Feng, R., Li, R., Zhang, L., et al. (2020). Unraveling the origin of moisture stability of halide solid-state electrolytes by in situ operando synchrotron X-ray analytical techniques. *Chem. Mater.* **32**, 7019–7027.

36. Nam, Y.J., Oh, D.Y., Jung, S.H., and Jung, Y.S. (2018). Toward practical all-solid-state lithium-ion batteries with high energy density and safety: comparative study for electrodes fabricated by dry- and slurry-mixing processes. *J. Power Sources* 375, 93–101.
37. Sakuda, A., Kuratani, K., Yamamoto, M., Takahashi, M., Takeuchi, T., and Kobayashi, H. (2017). All-solid-state battery electrode sheets prepared by a slurry coating process. *J. Electrochem. Soc.* 164, A2474–A2478.
38. Kato, Y., Shiotani, S., Morita, K., Suzuki, K., Hirayama, M., and Kanno, R. (2018). All-solid-state batteries with thick electrode configurations. *J. Phys. Chem. Lett.* 9, 607–613.
39. Hippauf, F., Schumm, B., Doerfler, S., Althues, H., Fujiki, S., Shiratsuchi, T., Tsujimura, T., Aihara, Y., and Kaskel, S. (2019). Overcoming binder limitations of sheet-type solid-state cathodes using a solvent-free dry-film approach. *Energy Storage Mater.* 21, 390–398.
40. Liu, Y., Zhang, R., Wang, J., and Wang, Y. (2021). Current and future lithium-ion battery manufacturing. *iScience* 24, 102332. <https://doi.org/10.1016/j.isci.2021.102332>.
41. Sakuda, A., Hayashi, A., Takigawa, Y., Higashi, K., and Tatsumisago, M. (2013). Evaluation of elastic modulus of $\text{Li}_2\text{S-P}_2\text{S}_5$ glassy solid electrolyte by ultrasonic sound velocity measurement and compression test. *J. Ceram. Soc. Jpn.* 121, 946–949.
42. Teflon PTFE Fluoropolymer Resin Properties Handbook. http://www.rjchase.com/ptfe_handbook.pdf.
43. Tan, D.H.S., Banerjee, A., Deng, Z., Wu, E.A., Nguyen, H., Doux, J., Wang, X., Cheng, J., Ong, S.P., Meng, Y.S., and Chen, Z. (2019). Enabling thin and flexible solid-state composite electrolytes by the scalable solution process. *ACS Appl. Energy Mater.* 2, 6542–6550.
44. Kurfer, J., Westermeier, M., Tammer, C., and Reinhart, G. (2012). Production of large-area lithium-ion cells – preconditioning, cell stacking and quality assurance. *CIRP Ann.* 61, 1–4.
45. Wang, C., Yu, R., Duan, H., Lu, Q., Li, Q., Adair, K.R., Bao, D., Liu, Y., Yang, R., Wang, J., et al. (2022). Solvent-free approach for interweaving freestanding and ultrathin inorganic solid electrolyte membranes. *ACS Energy Lett.* 7, 410–416.
46. Nam, Y.J., Cho, S.J., Oh, D.Y., Lim, J.M., Kim, S.Y., Song, J.H., Lee, Y.G., Lee, S.Y., and Jung, Y.S. (2015). Bendable and thin sulfide solid electrolyte film: a new electrolyte opportunity for free-standing and stackable high-energy all-solid-state lithium-ion batteries. *Nano Lett.* 15, 3317–3323.
47. Xu, R., Yue, J., Liu, S., Tu, J., Han, F., Liu, P., and Wang, C. (2019). Cathode-supported all-solid-state lithium-sulfur batteries with high cell-level energy density. *ACS Energy Lett.* 4, 1073–1079.
48. Schnell, J., Günther, T., Knoche, T., Vieider, C., Köhler, L., Just, A., Keller, M., Passerini, S., and Reinhart, G. (2018). All-solid-state lithium-ion and lithium metal batteries – paving the way to large-scale production. *J. Power Sources* 382, 160–175.
49. Doux, J.M., Nguyen, H., Tan, D.H.S., Banerjee, A., Wang, X., Wu, E.A., Jo, C., Yang, H., and Meng, Y.S. (2020). Stack pressure considerations for room-temperature all-solid-state lithium metal batteries. *Adv. Energy Mater.* 10, 1903253.
50. Kasemchainan, J., Zekoll, S., Spencer Jolly, D., Ning, Z., Hartley, G.O., Marrow, J., and Bruce, P.G. (2019). Critical stripping current leads to dendrite formation on plating in lithium anode solid electrolyte cells. *Nat. Mater.* 18, 1105–1111.
51. Lombardo, T., Duquesnoy, M., El-Bouysidy, H., Àren, F., Gallo-Bueno, A., Jørgensen, P.B., Bhowmik, A., Demortière, A., Ayerbe, E., Alcaide, F., et al. (2022). Artificial intelligence applied to battery research: hype or reality? *Chem. Rev.* 122, 10899–10969.
52. Lössberding, H., Wessel, S., Offermanns, C., Kehrer, M., Rother, J., Heimes, H., and Kampker, A. (2020). From cell to battery system in BEVs: analysis of system packing efficiency and cell types. *World Electr. Veh. J.* 11, 77.
53. Young, W.C.B., Richard, G.B., and Sadegh, A.M. (2012). *Roark's Formulas for Stress and Strain* (Mc Grow Hill).
54. Office of Energy Efficiency & Renewable Energy. (2020). Battery500: progress update. <https://www.energy.gov/eere/articles/battery500-progress-update>.

Joule, Volume 6

Supplemental information

**Scaling up high-energy-density sulfidic
solid-state batteries: A lab-to-pilot perspective**

Darren H.S. Tan, Ying Shirley Meng, and Jihyun Jang

Fig. S1. Cell to module conversion efficiency. Dimensions and relevant equations used in the calculations are shown below.

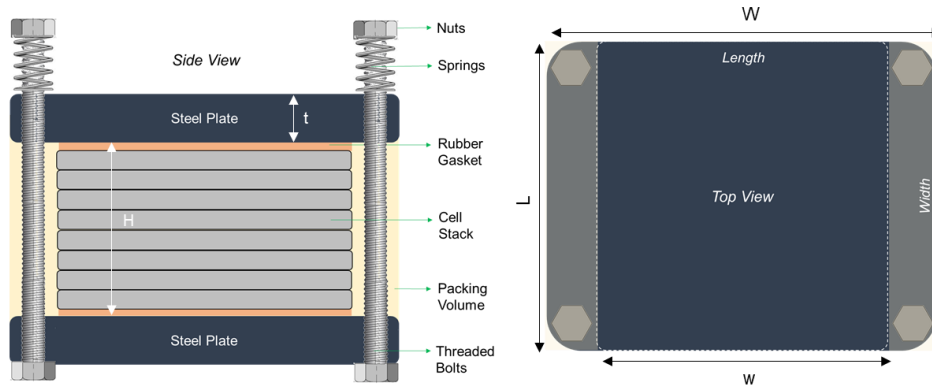


Plate thickness, $t = \left[\frac{aPL^4}{yE} \right]^{1/3}$

- a - Plate constant
- P - Pressure load applied / $N\ m^{-2}$
- L - Span length / m
- y - Deflection / mm
- E - Young's modulus / $N\ m^{-2}$

Conversion Efficiency, $\eta = \frac{m}{M+m}$ or $\frac{wLH}{WL(H+2t)}$

- m - Mass of cell stack
- M - Mass of module
- w - Width of cell stack
- W - Width of module
- H - Height of cell stack

Table S1. Cell parameters for energy density calculations.

	Baseline Half Cell	Graphite Full Cell	Thin SSE 30 μm	Thick Dry Electrode	100% Si Anode	Li Metal Anode	Anode Free
Nominal Voltage / V	3.125	3.7	3.7	3.7	3.35	3.75	3.75
Areal Capacity / mAh cm ⁻²	3	3	3	6	6	6	6
Np Ratio	5	1.2	1.2	1.2	1.2	1.2	-
Anode Capacity / mAh g ⁻¹	500	372	372	372	3500	3500	-
Anode Density / g cm ⁻³	7.3	2.3	2.3	2.3	2.3	0.5	-
Cathode Capacity / mAh g ⁻¹	200	200	200	200	200	200	200
Cathode Density / g cm ⁻³	2.4	2.4	2.4	2.4	2.4	2.4	2.4
SSE Thickness / μm	700	700	30	30	30	30	30
SSE Density / g cm ⁻³	1.6	1.6	1.6	1.6	1.6	1.6	1.6
SSE Relative Density / %	85	85	85	85	85	85	85
Cu Foil Thickness / μm	10	10	10	10	10	10	10
Cu Foil Density / g cm ⁻³	8.9	8.9	8.9	8.9	8.9	8.9	8.9
Al Foil Thickness / μm	10	10	10	10	10	10	10
Al Foil Density / g cm ⁻³	2.7	2.7	2.7	2.7	2.7	2.7	2.7
Binder Ratio / %	2	2	2	1	1	1	1